Structural, Electronic and Defect Properties of $Cu_2ZnSn(S,Se)_4$ Alloys

Shiyou Chen[1,2], Xin-Gao Gong[1], Aron Walsh[3], and Su-Huai Wei[4]
1Key Laboratory for Computational Physical Sciences (MOE) and Surface Physics Laboratory, Fudan University, Shanghai 200433, China
2Key Laboratory of Polar Materials and Devices (MOE), East China Normal University, Shanghai 200241, China
3Department of Chemistry, University College London, London WC1E 6BT, UK
4National Renewable Energy Laboratory, Golden, Colorado 80401, USA

ABSTRACT

Kesterite Cu_2ZnSnS_4 (CZTS) and $Cu_2ZnSnSe_4$ (CZTSe) compounds are candidate low-cost absorber materials for thin-film solar cells, and a light-to-electricity efficiency as high as ~10% has been achieved in the solar cell based on their alloys, $Cu_2ZnSn(S,Se)_4$ (CZTSSe). In this paper, we discuss the crystal and electronic structure of CZTSSe alloys with different composition, showing that the mixed-anion alloys keep the kesterite cation ordering, and are highly miscible with a small band gap bowing parameter. The phase stability of CZTS and CZTSe relative to secondary compounds such as ZnS and Cu_2SnS_3 has also been studied, showing that chemical potential control is important for growing high-quality crystals, and the coexistence of these secondary compounds is difficult to be excluded using X-ray diffraction technique. Both CZTS and CZTSe are self-doped to p-type by their intrinsic defects, and the acceptor level of the dominant Cu_{Zn} antisite is deeper than Cu vacancy. Relatively speaking, CZTSe has shallower acceptor level and easier n-type doping than CZTS, which gives an explanation to the high efficiency of CZTSSe based solar cells.

INTRODUCTION

In the past five years, the study about quaternary chalcogenide semiconductor Cu_2ZnSnS_4 (CZTS) has intensified, because CZTS is a strong candidate thin-film solar cell absorber material with the optimal band gap 1.5 eV and a high adsorption coefficient 10^4 cm^{-1}. [1-6] Compared to the currently used thin-film solar cell absorbers, e.g. ternary $CuInSe_2$ and binary CdTe, the advantage of CZTS is that all the constituent elements are naturally abundant and nontoxic, thus benefit the future large-area production with low cost of raw materials. CZTS can be derived from $CuInSe_2$ through replacing two In atoms by one Zn and one Sn, thus its crystal and electronic structure inherit the characters of $CuInSe_2$.[7,8] Due to the similarity between CZTS and $CuInSe_2$, CZTS-based solar cells can take the same device structure as $Cu(In, Ga)Se_2$ (CIGS) solar cells,[4] and it is expected that CZTS may substitute CIGS in the future.

Recently the alloys of CZTS and its Se counterpart $Cu_2ZnSnSe_4$ (CZTSe), which adopts the same crystal structure but has a smaller band gap (1.0 eV),[7] draw more and more attention. $Cu_2ZnSn(S,Se)_4$ (CZTSSe) thin film solar cell has achieved a light to electricity conversion efficiency as high as 10%,[9] which is currently the highest efficiency of CZTS related solar

cells. More recently, a group in Purdue University has fabricated CZTSSe nanocrystals based solar cell with an efficiency 7.2%, which is much higher than the efficiency 0.73% of CZTS nanocrystal based solar cell.[10,11] These successes indicate that CZTSSe alloys may be better solar cell absorber material than the CZTS compound, however, the reason is so far not clear. As we know, CZTS has the optimal band gap 1.5 eV for single-junction solar cells, and its alloying with CZTSe should decrease the band gap, deviating from the optimal value, which should decrease the efficiency, in contrast with the experimental findings. This abnormality is somewhat similar to the case in CIGS solar cells, where the efficiency approaches a maximum at low Ga content and starts to decrease if the Ga content is further increased, although the band gap becomes closer to the optimal gap value. To explain this abnormality, a clear understanding of the structural and electronic properties of CZTSSe alloys with different composition is necessary. However, although recent studies have addressed the structural and electronic properties of CZTS and CZTSe,[7,8,12,13] there is no detailed understanding of the CZTSSe alloys.

Besides the crystal and electronic structure, the defect properties are also important for explaining the compositional dependence of the solar cell efficiency. One important factor that leads to the high efficiency of CIGS solar cells is related with its special defect properties, e.g. the intrinsic defects in $CuInSe_2$ undergo self-passivation through forming defect complexes like $[In_{Cu}^{2+}+2V_{Cu}^{-}]$,[14] and the interface between the absorber layer and the CdS layer can be type-inverted to n-type,[15] which facilitates the separation of the electron-hole pairs. These special defect properties make CIGS solar cell exhibit electrically benign character and good performance, despite the poor crystallinity and serious non-stoichiometry. As we develop CZTSSe based solar cells, one natural question arises: do CZTS and CZTSe inherit the defect properties and electrically benign character from $CuInSe_2$.

To address these questions, we have performed first-principles calculations of the structural, electronic and defect properties for CZTSSe alloys, and studied their dependence on the composition. In the following, we will introduce our calculation methods first and then present our results in four separated sections.

CALCULATION METHODS

The total energy and band structure were calculated within the density functional formalism as implemented in the VASP code.[16] For the exchange-correlation potential, we used the generalized gradient approximation (GGA) of Perdew and Wang, known as PW91. Since the semi-local GGA usually underestimates the band gap of semiconductors significantly, we also calculate the band gaps employing a more sophisticated hybrid functional, the HSE (Heyd-Scuseria-Ernzerhof) functional in which one-quarter of Hartree-Fock nonlocal exchange interaction is added to the GGA functional, and a screening of $\mu = 0.2$ Å^{-1} is applied to partition

the exchange potential into short-range and long-range terms.[17] The d states of group IV elements are treated explicitly as valence. The interaction between the core electrons and the valence electrons is included by the frozen-core projector augmented wave method, and an energy cutoff of 300 eV was applied for the plane-wave basis set. For Brillouin-zone integration, we used k-point meshes that are equivalent to the $4\times4\times4$ Monkhorst-Pack meshes for an eight-atom cubic unit cell, and $2\times2\times2$ mesh for the 64-atom supercell. The convergence test shows that the increase of energy cutoff and k-points changes the band gap by less than 0.01 eV and the alloy formation energy by less than 0.1 meV/atom. All lattice vectors and atomic positions were fully relaxed by minimizing the stresses and forces.

To describe the random occupation of S and Se on the anion sites of the CZTSSe alloy, we use the special quasi-random structure (SQS) method in our calculation of the properties of alloys. To calculate the defect formation energy and transition-energy levels, we use the supercell approach in which a defect is placed in a 64-atom supercell. More details can be found in Ref. [18,19]

CRYSTAL STRUCTURE

According to our previous calculation, pure CZTS and CZTSe crystallize in the zinc-blende-derived kesterite structure as their ground state, with all cations ordered in one face-centered-cubic sublattice and all anions in another.[7,8] Besides kesterite structure, in CZTS and CZTSe the cations may adopt other ordering configuration as their metastable states, such as stannite structure and partially (Cu+Zn) disordered kesterite structure which has Cu and Zn cations in the (001) layers disordered due to the very low energy cost.[7,8]

Although kesterite is the lowest-energy structure for pure CZTS and CZTSe, it is not sure that kesterite still has lower energy when the anions S and Se are mixed in their sublattice. To study the energy stability of different cation-ordering configurations, we employ the SQS approach to mimic the random distribution of S and Se anions in a 64-atom supercell,[20,21] and calculate the formation enthalpy of $Cu_2ZnSn(S_{1-x}Se_x)_4$ alloys at different composition x,

$$\Delta H(x) = E(x) - (1-x)E_{CZTS} - xE_{CZTSe} \qquad (1)$$

where E_{CZTS} and E_{CZTSe} represent the total energy of pure CZTS and CZTSe in the kesterite structure, and E(x) is the total energy of the alloy with composition x. In Fig. 1, the black circles, blue triangles and red diamonds show the calculated formation enthalpy of the $Cu_2ZnSn(S_{1-x}Se_x)_4$ alloys with x=0, 0.25, 0.5, 0.75 and 1, and cations ordered in kesterite, stannite and partially disordered kesterite configurations respectively.

As we can see, the relative structural stability is not influenced by anion mixing and kept for alloys at all compositions over $0 < x < 1$; i.e., the energy increases in the following order: kesterite, disordered kesterite, and stannite. Furthermore, the energy differences between these

structures are kept almost constant at different compositions, e.g., 3–4 meV/atom between stannite and kesterite, and ~0.3 meV/atom between the partially disordered kesterite and kesterite. The small energy differences, especially for the partially disordered kesterite, indicate that these alternative configurations are likely to coexist in the synthesized alloys.

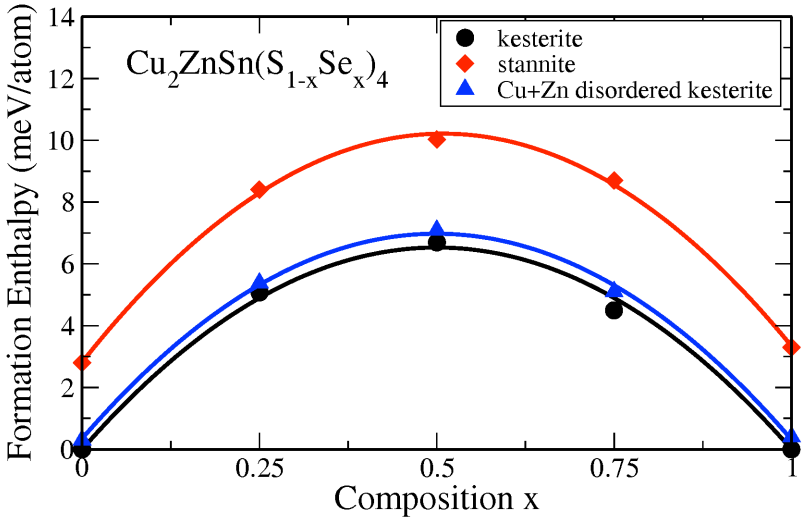

Figure 1. The calculated formation enthalpy of the $Cu_2ZnSn(S_{1-x}Se_x)_4$ alloy as a function of the composition x.[19] The cations are ordered in three different configurations.

According to the positive values of the formation enthalpy, the alloy prefers phase segregation into CZTS and CZTSe at zero temperature, and it costs additional energy to mix S and Se anions to form the random alloy. Usually the formation enthalpy obeys the following relation with the content x,

$$\Delta H(x) = (1-x)\Delta H(0) + x\Delta H(1) + \Omega x(1-x) \qquad (2)$$

where Ω is the interaction parameter that describes the cost of mixing. In Fig. 1, the lines show the fitting according to Equ. (2), and an interaction parameter of 26 meV/atom (or 52meV/mixed-atom) is got for the kesterite ordering. Compared to the larger interaction parameter (about 176 meV/mixed-atom) of $Cu(In_xGa_{1-x})Se_2$ (CIGS) alloys,[22] the small value of CZTSSe alloys indicate they are highly miscible, so we may expect the phase separation and alloy inhomogeneity of CIGS may not exist in CZTSSe alloys. Applying mean-field theory to the free energy of the solid solution, we estimate that the miscibility temperature of CZTSSe is less than 300 K, suggesting that it is stable at typical growth temperatures.

ELECTRONIC STRUCTURE

As derived from binary CdTe and ternary $CuInSe_2$, CZTS and CZTSe both have direct band gaps at Γ point, as shown in Fig. 2, where we plot the calculated band structure using the hybrid exchange-correlation functional. Although the band gap sizes are different, the overall shape of

the band structure of CZTS and CZTSe is very similar, which is easy to be understood since they have similar bonding (hybridization of atomic states) and crystal structure.

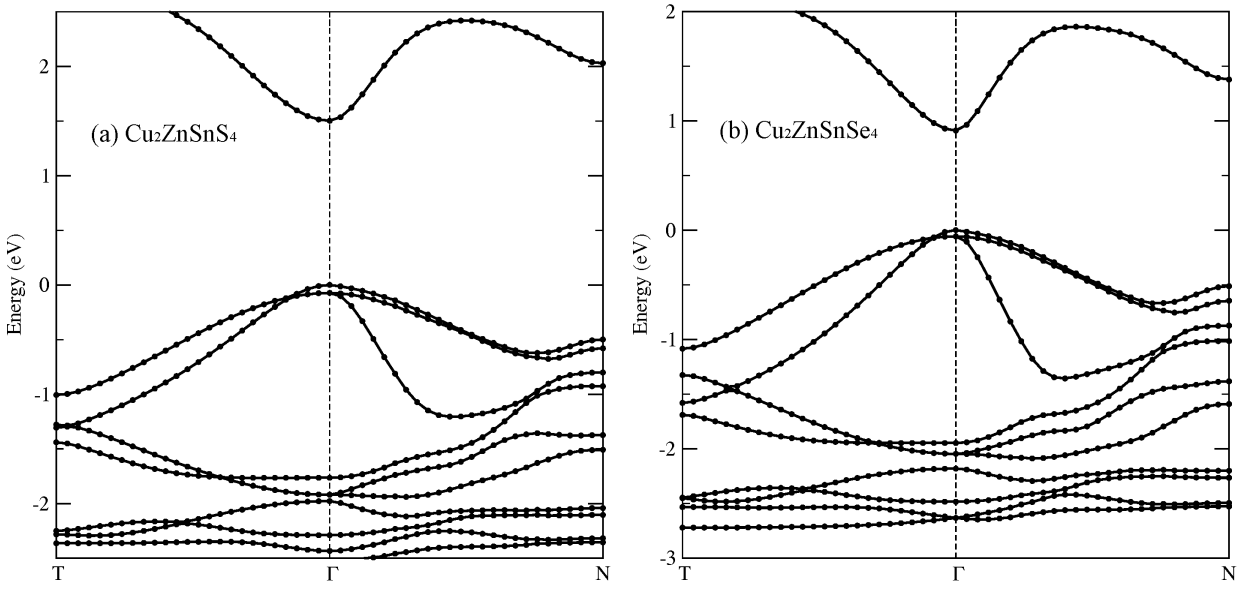

Figure 2. The calculated band structure using HSE exchange-correlation functional along the high symmetry lines T->Γ->N for (a) Cu_2ZnSnS_4 and (b) $Cu_2ZnSnSe_4$.

In Fig. 3, we plot the calculated band gaps of $Cu_2ZnSn(S_{1-x}Se_x)_4$ alloys with different composition x. The gap decreases monotonically when the Se content increases, from 1.5 eV at x=0 to 0.96 eV at x=1. As we can see, the decrease is almost linear; i.e., the band gap bowing parameter is small. The calculated band gap bowing (0.07 eV) of $Cu_2ZnSn(S_{1-x}Se_x)_4$ is similar to those of other mixed-anion alloys, $CuGa(S_{1-x}Se_x)_2$ (0.07 eV) and $CuIn(S_{1-x}Se_x)_2$ (0.04 eV), which results from the small size and chemical differences between S and Se.

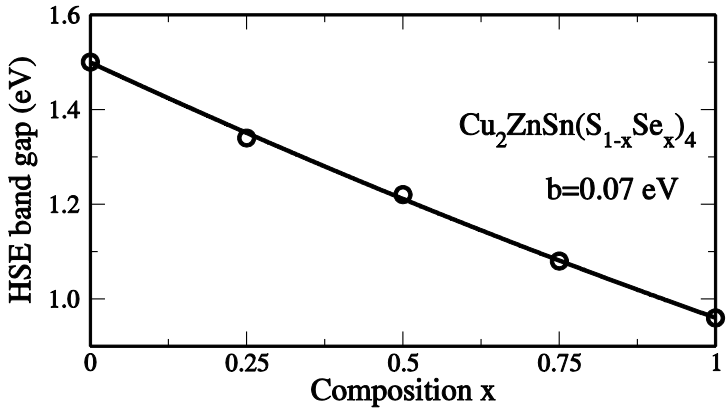

FIG. 3. The calculated band gap of $Cu_2ZnSn(S_{1-x}Se_x)_4$ at different composition x using the HSE functional.[19]

To demonstrate how the band gap decreases from CZTS to CZTSe, we have also calculated the band offset using a well-defined computational procedure.[18] As shown in Fig. 4, the band alignment between CZTSe and CZTS is of type I; that is, the valence band is higher and the conduction band is lower at the CZTSe side compared to CZTS.

This band alignment can be understood according to the nature of the valence band maximum (VBM) and the conduction band minimum (CBM) states:[19] (i) For Cu based chalcogenides including the quaternary Cu_2ZnSnS_4, $Cu_2ZnSnSe_4$ and ternary $CuInSe_2$, $CuGaSe_2$, the VBM is an antibonding state of the anion p and Cu d orbitals.[8,21] The S p level is lower than Se, thus the VBM of the sulfides is lower than that of the selenides; e.g., the VBM is 0.52 eV lower for ZnS than ZnSe, but the difference is reduced by p-d hybridization in Cu based chalcogenides, because the hybridization is stronger in the shorter Cu-S bond and pushes the antibonding VBM level of the sulfide up relative to that of the selenide. As a result, the valence band offset between Cu_2ZnSnS_4 and $Cu_2ZnSnSe_4$ is only 0.15 eV, and a similarly small offset exists between $CuGaS_2$ and $CuGaSe_2$, and $CuInS_2$ and CuInSe2. Since the p-d hybridization is similar for all Cu based selenides, their valence band offsets are smaller, as shown in Fig. 4. (ii) The CBM of Cu_2ZnSnS_4 and $Cu_2ZnSnSe_4$ is the antibonding state of the anion s and Sn s orbitals.[8] Although the s level of S is 0.2 eV lower in energy than Se, the shorter bond length of Sn-S makes the level repulsion stronger in Cu_2ZnSnS_4 and moves its CBM up relative to $Cu_2ZnSnSe_4$.

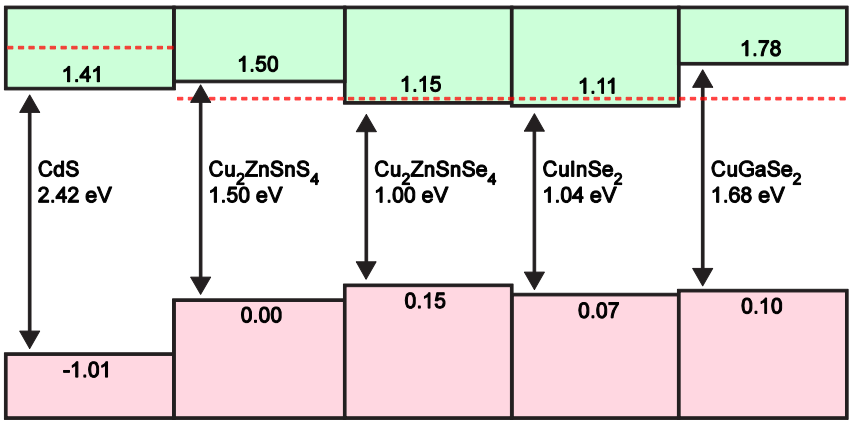

Figure 4. The calculated band alignment between CdS, Cu_2ZnSnS_4, $Cu_2ZnSnSe_4$, $CuInSe_2$, and $CuGaSe_2$ (the effects of spin-orbit coupling are included).[19] The red (dashed) line near the conduction band shows the pinning energy of the Fermi level for n-type doping.

From the larger conduction band offset (0.35 eV) than the valence band offset (0.15 eV), we expect that as the Se content increases in the $Cu_2ZnSn(S_{1-x}Se_x)_4$ alloy, the CBM downshift plays a more important role than the VBM upshift in the band gap decrease. As the band gap bowing is small, it is expected that the shift of band edge states is linear as a function of the composition x. The calculated band alignment and estimated band edge shift with the composition offer basic

parameters for the device simulation of CZTSSe based solar cells. Experimental verification of our calculated results is called for.

PHASE STABILITY

One important problem people have about the quaternary compound semiconductors is whether they can be synthesized experimentally, or are there any secondary phases coexisting in the synthesized samples? In fact, previous experiments about CZTS and CZTSe have shown that the coexistence of secondary phases, such as ZnS, Cu_2SnS_3, etc., non-stoichiometry and compositional non-uniformity are still challenges in the preparation of high-quality single phase CZTS and CZTSe compounds.[3,4,24-26] To theoretically understand their phase stability relative to the secondary compounds, we calculated the stability region in the chemical potential space, as shown in Fig. 5.

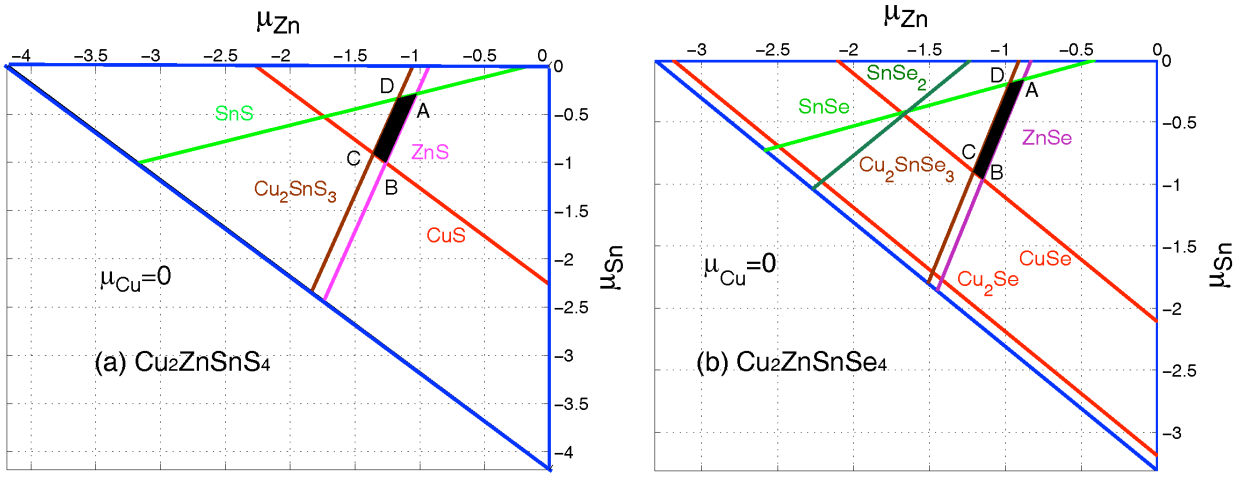

Figure 5. The calculated chemical-potential stable region of Cu_2ZnSnS_4 and $Cu_2ZnSnSe_4$ in the $\mu_{Cu}=0$ plane (the black area surrounded by A, B, C, and D points). All values are in eV.

The chemical potential μ_i is introduced to describe the richness of the element i, and $\mu_i=0$ means the element is so rich that their pure solid phase can form. Since the pure Cu, Zn, Sn metals and S, Se bulk are not allowed to exist in the synthesized samples, their chemical potentials are required to be negative. Besides the elemental bulk, secondary phases such as CuS, ZnS, SnS and Cu_2SnS_3 (similarly for selenides) are also not wanted, thus the following relations must be satisfied,

$$\mu_{Cu} + \mu_S < \Delta H_f(CuS) = -0.49\ eV$$
$$\mu_{Zn} + \mu_S < \Delta H_f(ZnS) = -1.75\ eV$$
$$\mu_{Sn} + \mu_S < \Delta H_f(SnS) = -1.01\ eV$$
$$2\mu_{Cu} + \mu_{Sn} + 3\mu_S < \Delta H_f(Cu_2SnS_3) = -2.36\ eV$$

Where ΔH_f means the calculated formation energy of the compounds. Similarly secondary phases such as Cu_2S, SnS_2, etc. also have limits to the chemical-potential stable region. To maintain a stable Cu_2ZnSnS_4 crystal, the chemical potential of Cu, Zn, Sn, and S must satisfy the following equation:

$$2\mu_{Cu} + \mu_{Zn} + \mu_{Sn} + 4\mu_S = \Delta H_f(Cu_2ZnSnS_4) = -4.21\,eV$$

This equation indicates only three of the four chemical potentials are independent; i.e. μ_S (μ_{Se} for CZTSe) is dependent on μ_{Cu}, μ_{Zn} and μ_{Sn}. Under the established constraints, the chemical-potential range of Cu, Zn, and Sn that stabilizes CZTS and CZTSe is bound in a polyhedron in the three-dimensional (μ_{Cu}, μ_{Zn} and μ_{Sn}) space. In Fig. 5 we plot the slices of the polyhedron in μ_{Cu}=0 eV plane. The black areas show the stable regions. As we can see, the stable regions are small for both CZTS and CZTSe, and a deviation from the stable region will cause the existence of CuS, ZnS, SnS or Cu_2SnS_3 (similarly for selenides). The narrow stable region shows that the chemical-potential control is very important for growing good-quality crystals. In particular, the stable region is very narrow along the μ_{Zn} axis, thus the content control of Zn should be taken very carefully. Experimentally, ZnS and Cu_2SnS_3 are observed in the samples,[24,25,27] which can be explained according to the narrow range of μ_{Zn}, i.e., Zn rich leads to ZnS while Zn too poor leads to Cu_2SnS_3.

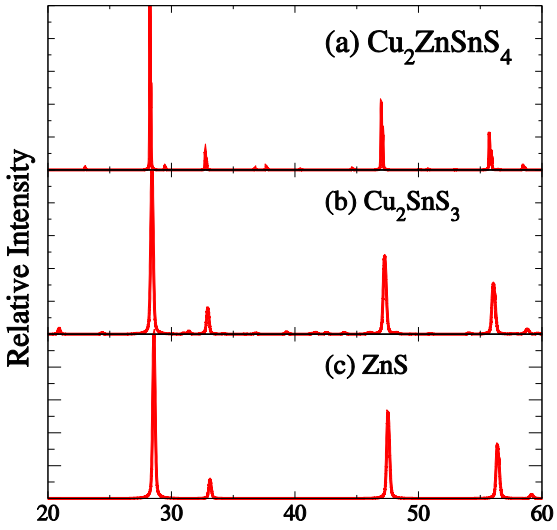

Figure 6. Simulated X-ray diffraction patterns of kesterite Cu_2ZnSnS_4, Cu_2SnS_3 with Cc symmetry and zinc-blende ZnS. The nominal X-ray source is Cu Kα (λ = 0.15406 nm).

In Fig. 6, we plot the simulated X-ray diffraction patterns of Cu_2ZnSnS_4, Cu_2SnS_3 and ZnS. It is obvious that the main peaks and their position are very similar for Cu_2ZnSnS_4 and the secondary compounds Cu_2SnS_3 and ZnS, which indicates that it is difficult to exclude the coexistence of these secondary phases using the X-ray diffraction technique,[26] especially considering that the quality of samples are currently still poor.

INTRINSIC DEFECTS

As quaternary compounds, Cu_2ZnSnS_4 and $Cu_2ZnSnSe_4$ have more intrinsic defects, such as vacancies, antisites and interstitials, than binary and ternary compounds. Which defect is dominant in the samples is quantitatively determined by the formation energy. In Fig. 7, we plot the calculated formation energies of different defects as function of the Fermi energy level. As the Fermi energy shifts up from the VBM to CBM, the formation energy of the negatively charged acceptors such as V_{Cu}, Cu_{Zn} and Zn_{Sn} decreases. When the formation energy of the charged defect is lower than that of the neutral one, the Fermi energy is called its transition energy level, shown by the filled circles in Fig. 7. In contrast with acceptors, the formation energy of positively charged donors, such as Zn_{Cu}, Cu_i and Sn_{Zn}, increases as the Fermi energy shifts up.

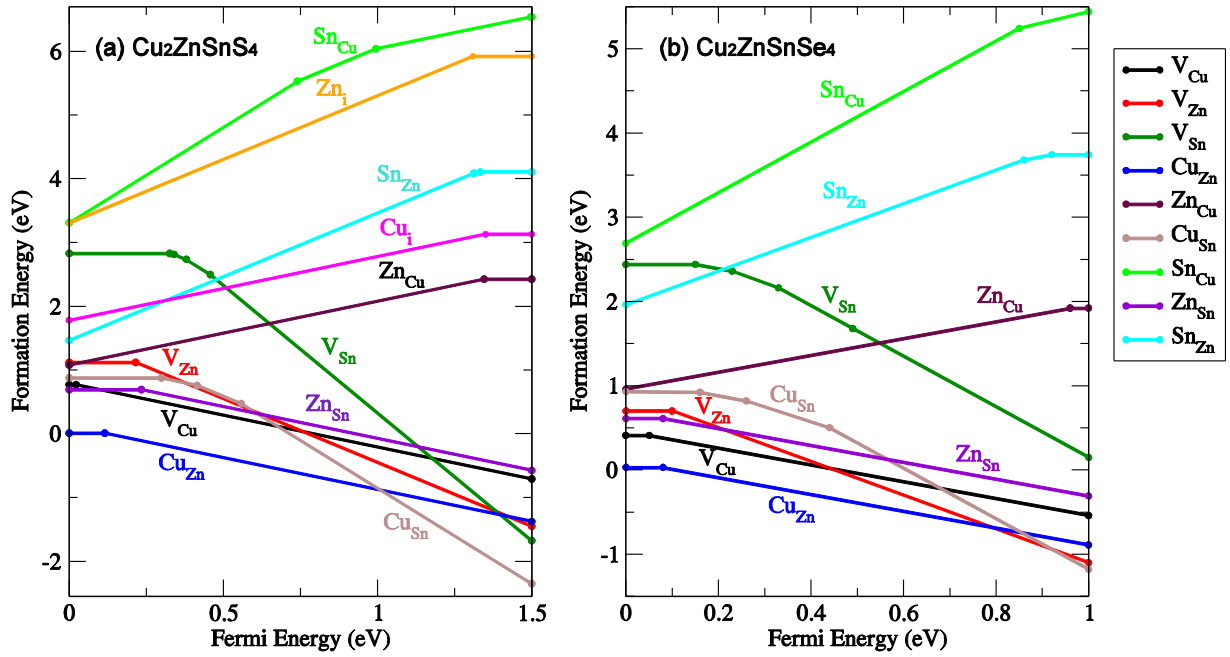

Figure 7. The change in the defect formation energy as a function of the Fermi energy at the chemical-potential point **A**. For each value of the Fermi energy only the most stable charge state is plotted with the filled circles representing a change in charge state (transition energy level).

In Fig. 7, two characters are clear, (i) the formation energies of most acceptors are lower than those of donors, explaining the experimentally observed p-type conductivity and indicating that the n-type doping is difficult in both compounds.[3] (ii) the lowest energy defect at the chemical-potential point A is Cu_{Zn} antisite, which is different from the case in ternary $CuInSe_2$ where the dominant defect is Cu vacancy. Because the energy differences of other acceptors (V_{Cu}, V_{Zn}, Zn_{Sn}, Cu_{Sn}) relative to the dominant Cu_{Zn} are not large (less than 1 eV), these defects may be formed in the samples too. The formation energy is also dependent on the chemical potential of

elements, so their relative stability and population in the samples can be tuned through changing the chemical potential condition during the synthesizing process.

In Fig. 8 we list the calculated transition energy levels in the band gap of Cu_2ZnSnS_4, which can be derived from Fig. 7. It is important to note that the dominant defect Cu_{Zn} has an acceptor level 0.12 eV above VBM, deeper than that of V_{Cu} (0.02 eV above VBM). The shallow level of V_{Cu} is common in Cu-based chalcopyrites like $CuInSe_2$ and $CuGaSe_2$. The deeper level of Cu_{Zn} can be explained by considering that the Cu on Zn antisite enhances the p-d hybridization between Cu and S. The deep level of the dominant defects is negative for CZTS solar cell efficiency, and we can decrease the formation energy and enhance the population of shallow V_{Cu} relative to Cu_{Zn} using Cu-poor and Zn-rich growth condition.[28] Experimentally this condition has been found to give high solar cell efficiency.[4,9,11]

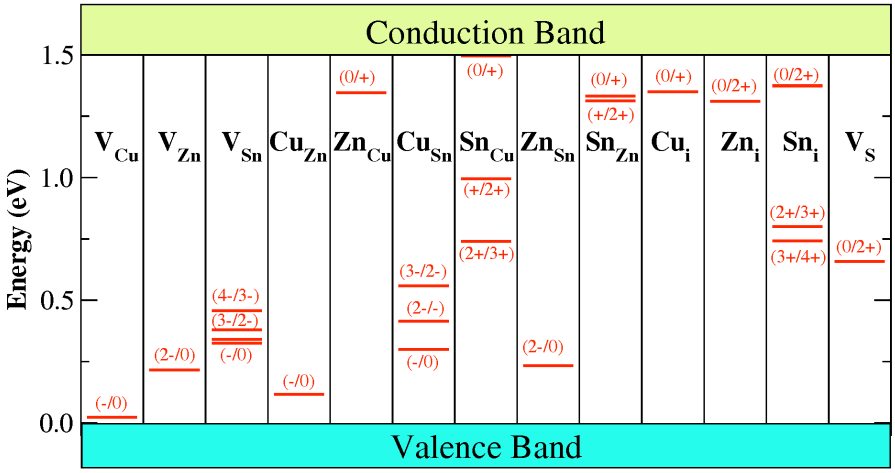

Figure 8. The transition-energy levels of intrinsic defects in the band gap of Cu_2ZnSnS_4.[18] The GGA band gap is corrected to the experimental value 1.5 eV, and the donor levels are shifted together with the CBM level.

Comparing the defect properties of Cu_2ZnSnS_4 and $Cu_2ZnSnSe_4$ (Fig. 7a and 7b), they have similar characters, i.e., acceptors have lower formation energy than donors, and Cu_{Zn} antisite is dominant with a deeper acceptor level. However, there are also differences, (i) the acceptor level is relatively shallower in $Cu_2ZnSnSe_4$, because the p-d hybridization between Cu and Se is weaker and its valence band is higher. (ii) the n-type doping should be easier in $Cu_2ZnSnSe_4$. According to the doping limit rules, a semiconductor is difficult to be doped to n-type if the conduction band level is too high, and is difficult to be doped to p-type if the valence band is too low in energy.[29] For n-type doping of I-III-VI_2 chalcopyrites, it has been shown that the Fermi energy level is pinned at about 0.06 eV above the CBM of $CuInSe_2$, indicating that a I-III-VI_2 semiconductor will be difficult to be doped to n-type if its CBM level is much higher than this pinning level. Since kesterite Cu_2ZnSnS_4 and $Cu_2ZnSnSe_4$ have similar electronic structure to

that of $CuInSe_2$, we can assume that the Fermi energy pinning level lines up for all chalcopyrite and kesterite compounds.[29] In Fig. 4, the red dashed line shows this pinning level. We can see that the line falls below the CBM level of Cu_2ZnSnS_4, while above that of $Cu_2ZnSnSe_4$, which indicates that the latter is relatively easier to be doped to n-type. The easier n-type doping make type-inversion to n-type possible at the surface of the p-type $Cu_2ZnSnSe_4$ absorber layer, which facilitates electron-hole separation of photo-generated carriers. Both the shallower acceptor level and easier n-type doping are positive factors for solar cell efficiency, which offers an explanation to the observed high efficiency of CZTSSe alloy based solar cells.

CONCLUSIONS

Using the first-principles calculation, we have studied the crystal and electronic structure, phase stability and defect properties of CZTSSe alloys with different composition. We find that, (i) the mixed-anion alloys keep the kesterite cation ordering, are highly miscible and have small band gap bowing. (ii) the chemical-potential stable region is narrow for CZTS and CZTSe, and the existence of the secondary compounds (ZnS and Cu_2SnS_3) cannot be excluded using X-ray diffraction technique. (iii) in both CZTS and CZTSe, most acceptors have lower formation energies than donors, and the acceptor level of the dominant Cu_{Zn} antisite is deeper than Cu vacancy, but CZTSe has shallower acceptor level and easier n-type doping than CZTS.

ACKNOWLEDGMENTS

The work is supported by the Natural Sciences Foundation (NSF) of China (Grants No. 10934002 and No. 10950110324) and Shanghai (Grant No. 10ZR1408800), the Research Program of Shanghai municipality and MOE, the Special Funds for Major State Basic Research, and the Fundamental Research Funds for the Central Universities. The work at NREL is funded by the US Department of Energy, under Contract No. DE-AC36-08GO28308.

REFERENCES

[1] A.Weber, S. Schmidt, D.Abou-Ras, P. Schubert-Bischoff, I. Denks, R. Mainz, and H. W. Schock, Appl. Phys. Lett. 95, 041904 (2009).

[2] K. Wang, O. Gunawan, T. Todorov, B. Shin, S. J. Chey, N. A. Bojarczuk, D. Mitzi, and S. Guha, Appl. Phys. Lett. 97, 143508 (2010).

[3] J. J. Scragg, P. J. Dale, L. M. Peter, G. Zoppi, and I. Forbes, Phys. Status Solidi B 245, 1772 (2008).

[4] H. Katagiri, K. Jimbo, W. S. Maw, K. Oishi, M. Yamazaki, H. Araki, and A. Takeuchi, Thin Solid Films 517, 2455 (2009).

[5] Y. K. Kumar, G. S. Babu, P. U. Bhaskar, and V. S. Raja, Solar Energy Materials and Solar Cells 93, 1230 (2009).

[6] A. Weber, H. Krauth, S. Perlt, B. Schubert, I. K¨otschau, S. Schorr, and H. Schock, Thin Solid Films 517, 2524 (2009).

[7] S. Chen, X. G. Gong, A. Walsh, and S.-H. Wei, Appl. Phys. Lett. 94, 041903 (2009).
[8] S. Chen, X. G. Gong, A. Walsh, and S.-H. Wei, Phys. Rev. B 79, 165211 (2009).
[9] T. K. Todorov, K. B. Reuter, and D. B.Mitzi, Adv. Mater. 22, E156 (2010).
[10] Q. Guo, H. W. Hillhouse, and R. Agrawal, J. Am. Chem. Soc. 131, 11672 (2009).
[11] Q. Guo, G. M. Ford, W. C. Yang, B. C. Walker, E. A. Stach, H. W. Hillhouse, and R. Agrawal, J. Am. Chem. Soc. 132, 17384 (2010).
[12] C. Perrson, J. Appl. Phys. 107, 053710 (2010).
[13] J. Paier, R. Asahi, A. Nagoya, and G. Kresse, Phys. Rev. B 79, 115126 (2009).
[14] S. B. Zhang, S.-H. Wei, A. Zunger, and H. Katayama-Yoshida, Phys. Rev. B 57, 9642 (1998).
[15] S.-H. Wei and S. B. Zhang, Phys. Rev. B 66, 155211 (2002).
[16] G. Kresse and J. Furthmuller, Phys. Rev. B 54, 11169 (1996).
[17] J. Heyd, G. E. Scuseria, and M. Ernzerhof, J. Chem. Phys. 118, 8207 (2003).
[18] S. Chen, J.-H. Yang, X. G. Gong, A. Walsh, and S.-H. Wei, Phys. Rev. B 81, 245204 (2010).
[19] S. Chen, A. Walsh, J.-H. Yang, X. G. Gong, L. Sun, P. X. Yang, J. H. Chu, and S.-H. Wei, Phys. Rev. B 81, 245204 (2010).
[20] S.-H. Wei, L. G. Ferreira, J. E. Bernard, and A. Zunger, Phys. Rev. B 42, 9622 (1990).
[21] S. Chen, X. G. Gong, and S.-H. Wei, Phys. Rev. B 75, 205209 (2007).
[22] S.-H. Wei and A. Zunger, J. Appl. Phys. 78, 3846 (1995).
[23] M. Gloeckler and J. Sites, Thin Solid Films 480-481, 241 (2005).
[24] S. Ahn, S. Jung, J. Gwak, A. Cho, K. Shin, K. Yoon, D. Park, H. Cheong, and J. H. Yun, Appl. Phys. Lett. 97, 021905(2010).
[25] K. Wang, B. Shin, K. B. Reuter, T. Todorov, D. Mitzi, and S. Guha, Appl. Phys. Lett. 98, 051912 (2011).
[26] W. Hass, T. Rath, A. Pein, J. Rattenberger, G. Trimmel, and F. Hofer, Chem. Commun. 47, 2050 (2011).
[27] T. Todorov, M. Kita, J. Carda, and P. Escribano, Thin Solid Films 517, 2541 (2009).
[28] S. Chen, X. G. Gong, A. Walsh, and S.-H. Wei, Appl. Phys. Lett. 96, 021902 (2010).
[29] S. B. Zhang, S.-H. Wei, and A. Zunger, J. Appl. Phys. 83, 3192 (1998).